ACS APPLIED MATERIALS & INTERFACES

www.acsami.org

Research Article

Generation and Characterization of a Library of Novel Biologically Active Functional Surfactants (Surfmers) Using Combined High-Throughput Methods

Valentina Cuzzucoli Crucitti, Leonardo Contreas, Vincenzo Taresco, Shaun C. Howard, Adam A. Dundas, Marion J. Limo, Takasi Nisisako, Philip M. Williams, Paul Williams, Morgan R. Alexander, Ricky D. Wildman,* Benjamin W. Muir,* and Derek J. Irvine*

Cite This: https://doi.org/10.1021/acsami.1c08662

Read Online

ACCESS | Metrics & More | Article Recommendations | Supporting Information

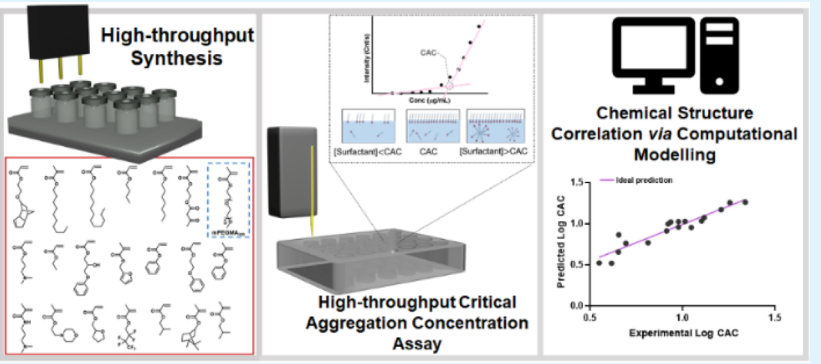

ABSTRACT: We report the first successful combination of three distinct high-throughput techniques to deliver the accelerated design, synthesis, and property screening of a library of novel, bio-instructive, polymeric, comb-graft surfactants. These three-dimensional, surface-active materials were successfully used to control the surface properties of particles by forming a unimolecular deep layer on the surface of the particles via microfluidic processing. This strategy deliberately utilizes the surfactant to both create the stable particles and deliver a desired cell-instructive behavior. Therefore, these specifically designed, highly functional surfactants are critical to promoting a desired cell response. This library contained surfactants constructed from 20 molecularly distinct (meth)acrylic monomers, which had been pre-identified by HT screening to exhibit specific, varied, and desirable bacterial biofilm inhibitory responses. The surfactant's self-assembly properties in water were assessed by developing a novel, fully automated, HT method to determine the critical aggregation concentration. These values were used as the input data to a computational-based evaluation of the key molecular descriptors that dictated aggregation behavior. Thus, this combination of HT techniques facilitated the rapid design, generation, and evaluation of further novel, highly functional, cell-instructive surfaces by application of designed surfactants possessing complex molecular architectures.

KEYWORDS: *surfactant, high throughput, polymerization, critical aggregation concentration, CAC*

1. INTRODUCTION

The rise of combinatorial chemistry approaches and high-throughput (HT) methods represent a significant breakthrough in the contemporary design and screening of new materials.[1−4] They have been demonstrated to be highly important tools in the development of libraries of novel chemistry/materials, where the functional properties of new products cannot easily be predicted from current empirical data. Polymer chemistry is highly suitable for the application of these HT methods due to the variety of parameters that can be systematically altered, for example, monomer types, initiators, catalysts, solvents, reaction temperatures, and order of reagent addition.[5−7] In this case, the application of HT combinatorial synthesis/screening approaches allows the rapid discovery of polymeric candidates that exhibit specific targeted chemical, physical, and biological properties, while using very small reagent volumes, thereby saving significant time, materials, and labor.[8−12] For example, our combinatorial screening has delivered significant advances in the field of biomaterials,

Received: May 10, 2021
Accepted: July 19, 2021

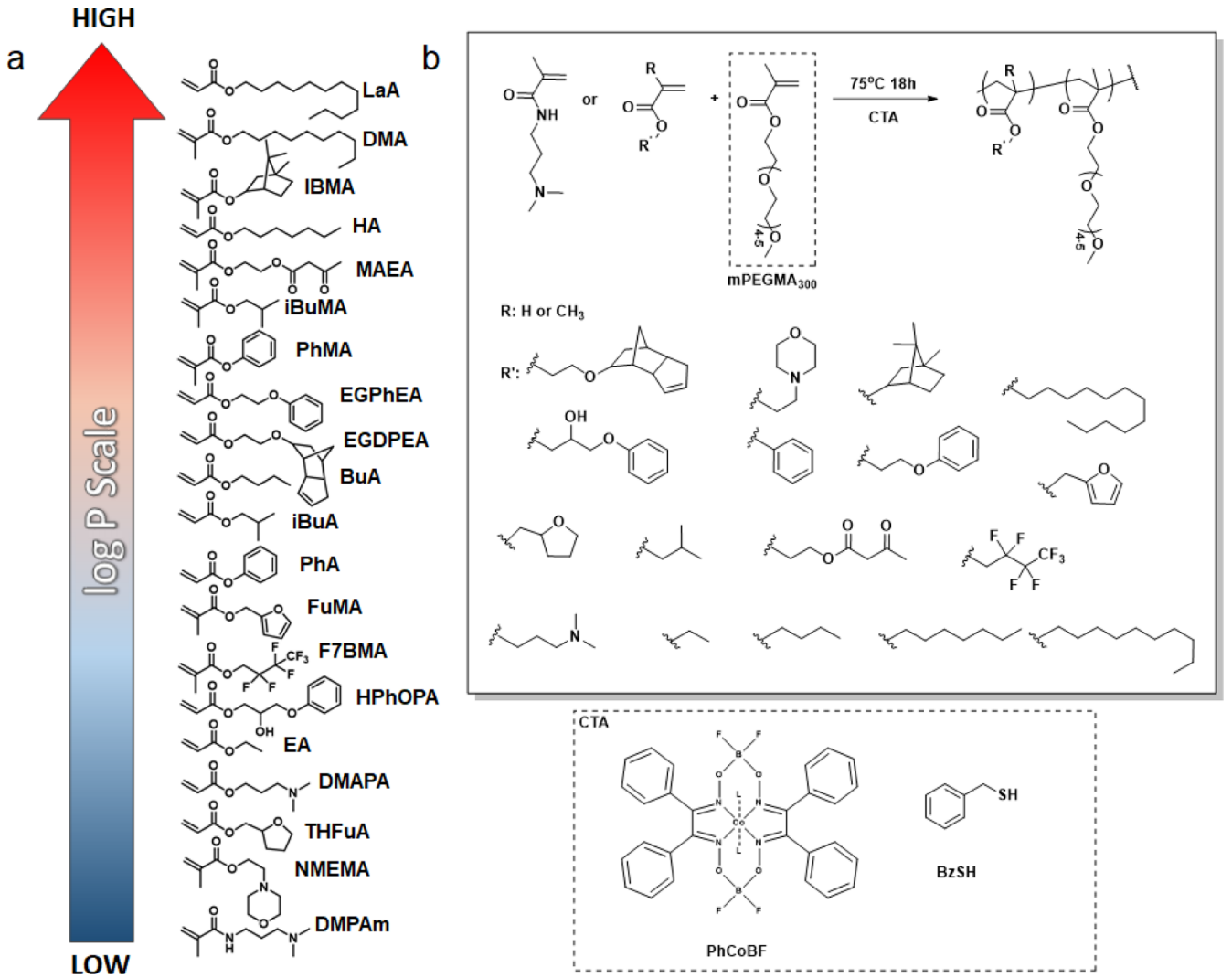

Figure 1. (a) Library of 20 hydrophobic monomers employed in the HT synthesis with mPEGMA300 (clog *P* values are reported in Table S1). (b) Reaction scheme for free-radical polymerization controlled by two different CTAs: PhCoBF and benzyl mercaptan.

including the discovery of (a) new poly(meth)acrylates that are able to support stem cell expansion and differentiation[13−15] and resist fungal colonization of surfaces[16] /prevent bacterial biofilm formation without killing the entities that contact the surface[17] and (b) novel methods to predict formulations that will deliver gel formation/creation of dual-network materials.[18] Furthermore, these studies have led to a commercialized product in the form of a CE-marked urinary catheter.[19]

Free-radical polymerization is of particular interest for HT screening since it does not necessarily require stringent process conditions/pre-preparation of reagents and can be used for the (co)polymerization of a wide range of vinyl monomers, including (meth)acrylates, (meth)acrylamides, styrenyls, and so forth.[20] Consequently, there have been several reports in the literature of successful examples of HT processing using controlled radical polymerization (CRP) techniques, such as reversible addition−fragmentation chain transfer and atom transfer radical polymerization.[8,21,22] However, the multi-component complexity of the mechanisms and the high cost of the reagents needed for these types of chemistries have made it difficult to use HT processes as part of a scalable design. In contrast, most commercial polymerization processes achieve reaction control via the use of less complex systems which adopt single-event chain-transfer agents (CTAs),[17,20,21] for example, thiols. Alternatively, catalytic chain-transfer polymerization (CCTP) has been shown to exhibit very high levels of molecular weight control on a commercial scale, while using very small quantities (ppm) of cobalt-based catalytic CTAs.[23−30]

Herein, we report, for the first time, the successful use of two chain-transfer mechanisms to control radical polymerization (i.e., thiol-mediated radical polymerization and CCTP) within an HT synthesis process to develop a library of novel functional amphiphilic, polymeric surfactants (Figure 1a,b).

Surfactants, due to their amphiphilic character, have a huge versatility in terms of their end-use applications as they are fundamental to successfully delivering a variety of technologies, for example, the formation of emulsions, personal care products, and dispersed systems.[31,32] Recently, both the development of new CRP synthetic pathways[33−35] and/or the need to develop new functional materials with specific biological activities have increased interest in these highly functional materials.[36−39] However, while they are often necessary in order to create structures that are essential to these applications, for example, responsible for the formation

https://doi.org/10.1021/acsami.1c08662
ACS Appl. Mater. Interfaces XXXX, XXX, XXX−XXX

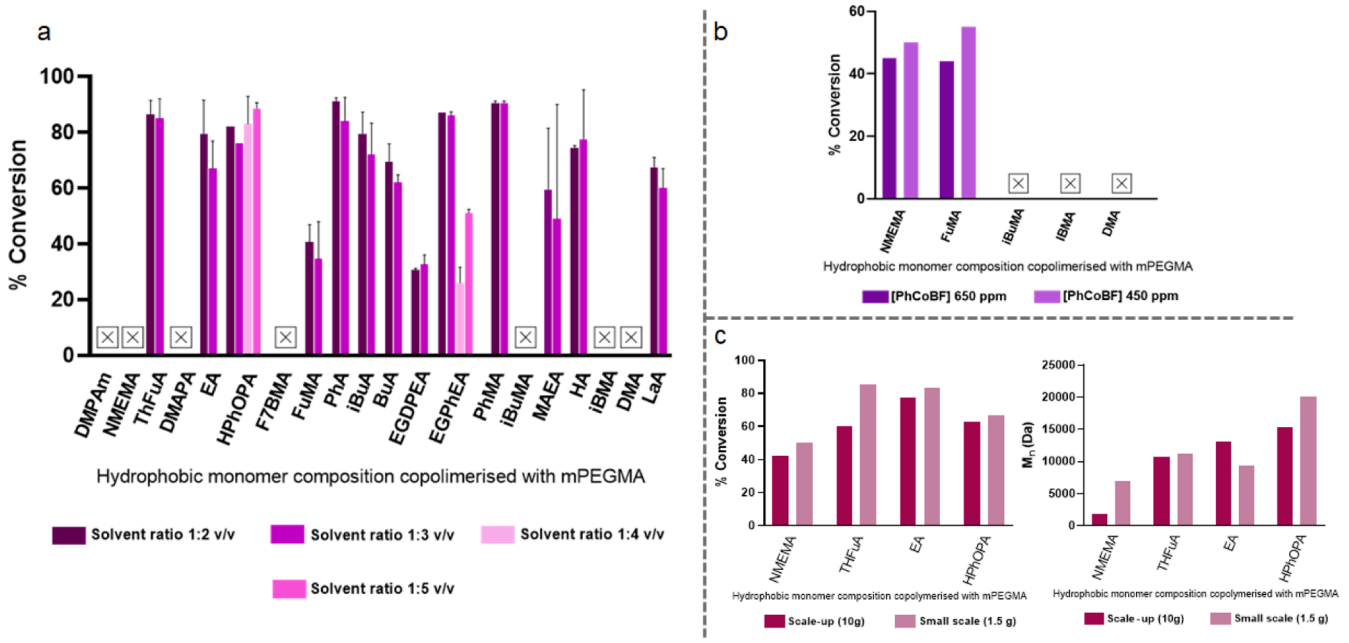

Figure 2. (a) % Conversion determined by ^{1}H NMR while varying the solvent/monomer ratio determined by ^{1}H NMR. (b) % Conversions from a further screen using a reduced catalyst concentration (650 and 450 ppm) determined by ^{1}H NMR. (c) Comparison of the % conversion and M_n between the small scale (1.5 g) and large scale (10 g) determined by ^{1}H NMR and GPC, respectively. The crossed boxes indicate monomers where no conversion was observed.

of micelles, their presence in a final formation can be detrimental to its end-use performance.

This paper details a novel approach to the application of such amphiphilic materials such that they not only are responsible for the formation of the desired structure but also deliver the primary biological function at the structure's surface. The report demonstrates the use of specific surfactant designs based upon the data mining of HT data sets to control the biological properties of the first monolayer of the resultant material/particle surface structure. In this way, the use of the surfactant becomes highly desirable and additive to the final particle performance. Furthermore, from a commercial perspective, this strategy limits both (a) the quantity of the typically more costly, functional monomers required to construct the surfactant and (b) its influence upon the particle's material properties. Rather, the bulk or core material can dictate the macro-material properties of the particles, for example, degradability and mechanical/material characteristics, allowing these properties to be tuned by simply changing the core monomer, while keeping the surfactant, and so biological performance, the same. The control of surfactant functional properties has been exemplified by evaluating their critical aggregation concentration (CAC) using a new HT method.

2. RESULTS AND DISCUSSION

This paper reports the first application of the efficient, robust, versatile, and industrially applicable CCTP methodology to the copolymerization of a range of (meth)acrylate monomers when adopting an HT synthesis methodology. The aim was to produce a library of structurally differentiated, bio-instructive amphiphilic polymeric surfactants.[40−42] In particular, this study broadens the nature of the hydrophobic, bio-instructive monomers used to allow the design optimization of target polymeric surfactants (i.e., surfmers) for both (a) delivery of specific bioactivity and (b) application in microfluidic processing to both generate micelles and deliver a unimolecular coating of bio-instructive materials and as such extends the work reported in a prior paper by the authors.[43] Specifically, the (meth)acrylate monomers chosen in this work were previously screened and shown to exhibit positive bio-instructive performance. For example, some demonstrated increased attachment/proliferation of human cells (i.e., cardiomyocytes and human pluripotent stem cells) and others inhibited bacterial attachment and biofilm formation (e.g., *Pseudomonas aeruginosa, Staphylococcus aureus,* and *Escherichia coli*).[15,17,44] The palette of (meth)acrylate-based hydrophobic monomers (HbMs) used to generate this library of functional polymeric surfactants was chosen to include a variety of functional groups (e.g., benzyl, alkyl, fluorine, amine, and so forth) and incorporate a range of hydrophobicities based on their calculated log *P* values (i.e., clog *P*), where ALOGPS 2.1 online software was used for the calculation of the clog *P* values.[45−47]

2.1. Feasibility Scale Screening (1.5 g) HT CCTP Polymerizations. *2.1.1. HT Optimization for Molecular Structure Synthesis.* In the first sequence of copolymerizations, an initial screen was performed to study how the hydrophobic monomer library responded to CCTP catalytic control. Part of the screening involved varying the solvent ratios from 1/2 to 1/3 v/v (mon/solvent) to determine whether the concentration of the reaction mixture affected the final composition of the polymers, especially in terms of molecular weight. Moreover, in the case of the HPhOPA-*co*-mPEGMA300 and EGPhEA-*co*-mPEGMA300 copolymers, additional monomer/solvent ratios (1/4 and 1/5 v/v) were explored because of the high viscosity exhibited by the starting materials.

These first CCTP reaction screening experiments resulted in the successful HT synthesis of a library of copolymers from 13 of the HbMs (Figure 2a) that exhibited the desired target molecular structure. In the majority of cases, the conversion was 50% or greater, which provided sufficient material to allow

https://doi.org/10.1021/acsami.1c08662
ACS Appl. Mater. Interfaces XXXX, XXX, XXX−XXX

Table 1. M_n, $Đ$, Final Copolymer (Hydrophobic Monomer (HbM)/mPEGMA300) Ratio for the CCTP Initial Screening and Optimization with mPEGMA300 Using a Feed Ratio of 90/10 mol/mol, Different Solvent Ratios, and Different Catalyst Concentrations

entry	HbM	clog P	solvent monomer ratio [v/v]	PhCoBF (ppm)	M_n[a] (kDa)	$Đ$[a]	final HbM/PEG ratio[b] [mol/mol]
1	NMEMA	0.47	3:1	650	2.55	1.50	88:12
2	NMEMA		3:1	450	1.77	1.77	93:7
3	THFuA	1.01	2:1	850	14.69	2.18	94:6
4	THFuA		3:1	850	10.64	2.45	91:9
5	EA	1.24	2:1	850	18.21	2.23	90:10
6	EA		3:1	850	13.04	2.46	88:12
7	HPhOPA	1.94	2:1	850	25.3	3.58	89:11
8	HPhOPA		3:1	850	15.31	3.76	91:9
9	HPhOPA		4:1	850	13.13	2.84	90:10
10	HPhOPA		5:1	850	15.00	3.61	91:9
11	FuMA	2.01	2:1	850	0.94	1.19	87:13
12	FuMA		3:1	850	0.99	1.20	87:13
13	PhA	2.08	2:1	850	16.71	2.47	89:11
14	PhA		3:1	850	12.88	2.56	88:12
15	iBuA	2.14	2:1	850	17.82	2.64	89:11
16	iBuA		3:1	850	15.00	2.71	89:11
17	BuA	2.20	2:1	850	10.7	2.16	88:12
18	BuA		3:1	850	14.34	2.24	89:11
19	EGDPEA	2.28	2:1	850	7.26	2.27	91:9
20	EGDPEA		3:1	850	4.40	2.19	87:13
21	EGPhEA	2.33	2:1	850	29.3	3.70	93:7
22	EGPhEA		3:1	850	14.50	3.73	88:12
23	EGPhEA		4:1	850	6.46	2.24	87:13
24	EGPhEA		5:1	850	9.32	2.19	89:11
25	PhMA	2.48	2:1	850	3.00	2.48	94:6
26	PhMA		3:1	850	2.50	2.54	92:8
27	MAEA	2.85	2:1	850	1.50	1.21	68:32
28	MAEA		3:1	850	1.20	1.16	63:37
29	HA	3.27	2:1	850	20.66	2.90	93:7
30	HA		3:1	850	15.42	1.90	93:7
31	LaA	6.13	2:1	850	18.54	2.29	96:4
32	LaA		3:1	850	13.50	2.80	87:13

[a]M_n and $Đ$ were calculated by GPC. [b]Final copolymer ratios were calculated by ^{1}H-NMR.[53]

further analysis and testing. However, seven of the hydrophobic monomers (DMPAm, DMAPA, F7BMA, DMA, iBMA, iBuMA, and NMEMA) did not form any copolymers or produced yields less than 30% under these initial conditions. Three potential causes were identified for this disruption of the CCTP mechanism: (a) the presence of moieties in the monomer which prevented the necessary change in the transition state of the cobalt complex,[48,49] (b) the reactivity of the monomer was so low that the PhCoBF preferentially interacted with the newly generated radical prior to it being involved in initiation, and/or (c) the relatively high PhCoBF concentration (850 ppm), chosen to improve the conversion of the less reactive acrylates present in the series, may have inhibited polymerization of the methacrylates.[50,51] Thus, a relatively high PhCoBF concentration (850 ppm) had been chosen in the standard polymerization procedure due to the greater number of acrylate monomers present in the test series, which is known to cause inhibition of the free-radical reaction when methacrylates are involved.[50]

In light of the aforementioned hypothesis (c), a second series of copolymerizations were conducted with the methacrylate monomers from the CCTP "failure" subset (i.e., NMEMA, iBMA, iBuMA, and DMA) and included FuMA as it had a low yield in the initial screen. These were conducted with reduced CTA concentrations, 650 and 450 ppm (Figure 2b).

The results from these copolymerizations separated into two groups with both FuMA-*co*-mPEGMA300 and NMEMA-*co*-mPEGMA300 showing a net improvement in the yield achieved with 450 ppm of the catalyst. The former increased from ∼30% with 850 ppm to ∼60% using 450 ppm of the catalyst, while the conversion of the latter reached up to 50% with 450 ppm. Thus, it was concluded that these reactions were retarded due to low monomer reactivity. By comparison, the iBMA-, iBuMA-, and DMA-*co*-mPEGMA300 copolymerization still did not form a polymer under these reduced CTA regimes. Thus, their lack of reactivity was attributed to steric hindrance from the large pendant groups that are directly attached to the chain (i.e., no flexible spacer group is present), encouraging a combination of (a) enhanced radical stability and (b) reduced chain end reactivity with the complex, thereby encouraging PhCoBF to interact directly with the initiator radical prior to initiation.[52]

Due to the screening nature of the work contained in this study, a fundamental investigation into specific monomer reactivity behavior that was exhibited within the HT strategy was considered beyond the scope of the work. These reactivity observations, which are thought to relate to factors such as

https://doi.org/10.1021/acsami.1c08662
ACS Appl. Mater. Interfaces XXXX, XXX, XXX−XXX

Table 2. Conversion, M_n, $Đ$, Final Copolymer Ratio, and Conversion Data for the Hydrophobic Monomers (HbM): iBMA, iBuMA, DMA, DMAPA, DMPAm, and F7BMA-Based mPEGMA300 Copolymers Using Thiol-Mediated Free-Radical Polymerization with a Target Feed Ratio of 90/10 mol/mol

entry	HbM/mPEGMA300	BzSH [% mol] (%)	M_n[a] [kDa]	$Đ$[a]	final HbM/PEG ratio[b] [mol/mol]	% conv[b]
1	iBMA	5	7.10	1.44	92:8	87
2	iBMA	10	3.60	1.43	93:7	85
3	iBuMA	5	6.88	1.67	N/A	90
4	iBuMA	10	4.92	1.43	N/A	88
5	DMA	5	5.40	1.43	93:7	80
6	DMA	10	3.00	1.39	92:8	86
7	DMAPA	5	8.70	1.48	95:5	90
8	DMAPA	10	7.22	1.45	93:7	84
9	DMPAm	5	6.50	2.4	86:14	90
10	DMPAm	10	4.11	2.65	89:11	92
11	F7BMA	5	6.31	1.2	92:8	90
12	F7BMA	10	5.21	1.2	93:7	88

[a]M_n and $Đ$ were calculated by GPC. [b]Final copolymer ratios were calculated by ^{1}H-NMR.[53]

catalyst solubility/comparability within the reaction mixture, monomer solution viscosity, and so forth are now under investigation in more mechanistic detail.

2.1.2. CCTP Screen Copolymer Characterization. The M_n obtained for the majority of the copolymers varied between 1.5 and 15 kDa, which was within the targeted range (Table 1).

In addition to the hydrophobic monomer type, the initial screen also investigated the effect of monomer concentration, where varying the monomer/solvent ratio from 1/3 to 1/2 v/v was noted to affect the M_n, with the most concentrated conditions producing an increase in the M_n of up to 30%. This may be due to a higher rate of chain transfer to the solvent or that CTA is less likely to meet a chain end under the dilute conditions. Meanwhile, the variation of the solvent/monomer ratio did not significantly alter the final values of $Đ$ of the product surfactants. Typically, the copolymers bearing a hydrophobic methacrylate comonomer (PhMA, NMEMA, and FuMA) exhibited lower M_n values of around 2 kDa, even when lower CTA concentrations were applied, confirming that the chain-transfer process from the catalyst worked more efficiently with these monomers.

Table 1 also contains the final molar composition of these materials; this defines the balance between the hydrophilic and hydrophobic moieties and so the ability of the surfactant to self-assemble. The final copolymer ratios, that is, the final relative monomer compositions inside the polymer backbone, were determined via ^{1}H NMR analysis of the purified copolymers and showed that all the surfactants were close to the feed ratio target range, that is, within the range of 80/20 to 95/5, with the exception of MAEA-*co*-mPEGMA300. This particular surfactant exhibited a hydrophobic monomer/mPEGMA300 ratio of around 68/32. This was attributed to the fact that there are multiple double bonds in this monomer structure, potentially presenting several potential sites for the radical to interact with.

The characterization data in Table 1 identified that CCTP was a versatile method for the polymerization of a wide range of acrylates/methacrylates and demonstrated that it is a robust process broadly applicable to HT methods, thus capable of generating copolymer libraries. However, it was noted that the monomers with multiple double bonds studied in this work are a potential exception for the reasons given above.

2.2. Up-Scaled Screening (10 g) HT CCTP Polymerizations. A scalability screen to investigate the scale-up of the CCTP-based HT copolymerizations from 1 to 10 mL was then conducted on a subset of four polymers as a proof-of-concept study. The four polymers were selected based on their chemical functionalities and the experimental conditions required to synthesize them on a small scale. THFuA-*co*-mPEGMA300 and EA-*co*-mPEGMA300 were chosen because they contained an acrylate group. HPhOPA-*co*-mPEGMA300, while also an acrylate, exhibited high viscosity and thus required a monomer/solvent ratio of 1/5 v/v. Finally, NMEMA-*co*-mPEGMA300 was included both as a representative methacrylate and because of its amine pendant group. This scale-up experiment was conducted employing the same reaction conditions previously adopted during feasibility screening without further optimization. The data confirmed the robustness of the CCTP process, when applied at a larger scale, as without any specific alterations under reaction conditions, almost identical M_n (Figure 2c) and reactivity ratios and a high conversion in the final product were retained (Figure 2c). These results are reported in detail in Table S2.1.

2.3. Feasibility (1.5 g) Scale HT Thiol-Mediated Free-Radical Polymerization. A second industrially exploited CTA, benzyl mercaptan (BzSH), was employed to further investigate the hypothesis that the "failure" of some CCT-based HT polymerizations was due to intrinsic limitations of the control method rather than a flaw with the automated process. This model thiol CTA was added at two different concentrations: 5 and 10% mol/mol relative to the monomers. The hydrophobic monomers used for this sequence of experiments were DMPAm, DMAPA, DMA, F7BMA, iBMA, and iBuMA, and the monomer/solvent ratio adopted was 1/3 v/v. Typically, the thiol-mediated polymerization produced hydrophobic monomer-*co*-mPEGMA300 copolymers at high conversions, ∼80−85%, at both BzSH feed concentrations (Table 2).

The exception was the DMPAm-*co*-mPEGMA300 copolymer that only achieved an ∼55% conversion, which was still above the targeted level set. This may be linked to poor reactivity between the hydrophobic monomer and the thiol due to the presence of the amine group. The M_n achieved ranged from 3 to 13.4 kDa (Table 2), again within the targeted range. Unfortunately, in the case of iBuMA-*co*-mPEGMA300, it was not possible to separate the polymer from the reaction mixture via non-solvent precipitation, so further characterization could not be performed. The M_n values were noted to

https://doi.org/10.1021/acsami.1c08662
ACS Appl. Mater. Interfaces XXXX, XXX, XXX−XXX

Table 3. CACs and Size of the Surfactant Aggregates Obtained from the HT Method Using Either CCTP or Thiol-Mediated Free-Radical Polymerization[a]

entry	copolymer	CAC [μg/mL]	size at the CAC [nm]	size above CAC [nm]	final HbM/PEG ratio
1	(EGDPEA-*co*-mPEGMA)$_{CCTP}$	8.4	122	110	87:13
2	(iBMA-*co*-mPEGMA)$_{BzSH}$	5.0	103	104	92:8
3	(PhA-*co*-mPEGMA)$_{CCTP}$	10.3	180	183	88:12
4	(THFuA-*co*-mPEGMA)$_{CCTP}$	11	249	247	91:9
5	(MAEA-*co*-mPEGMA)$_{CCTP}$	20.0	158	146	63:37[b]
6	(BuA-*co*-mPEGMA)$_{CCTP}$	9.5	161	167	89:11
7	(EA-*co*-mPEGMA)$_{CCTP}$	13.0	157	150	88:12
8	(LaA-*co*-mPEGMA)$_{CCTP}$	4.0	199	196	87:13
9	(F7BMA-*co*-mPEGMA)$_{BzSH}$	18.0	98	71	93:7
10	(DMPAm-*co*-mPEGMA)$_{BzSH}$	16.1	124	135	86:14
11	(HA-*co*-mPEGMA)$_{CCTP}$	8.2	88	96	93:7
12	(DMAPA-*co*-mPEGMA)$_{BzSH}$	22.0	103	101	95:5
13	(FUMA-*co*-mPEGMA)$_{CCTP}$	9.5	216	231	92:8
14	(DMA-*co*-mPEGMA)$_{BzSH}$	4.5	170	163	93:7
15	(PhMA-*co*-mPEGMA)$_{CCTP}$	9.0	274	365	92:8
16	(iBuA-*co*-mPEGMA)$_{CCTP}$	4.5	109	102	89:11
17	(NMEMA-*co*-mPEGMA)$_{CCTP}$	13.0	218	220	93:7
18	(HPhOPA-*co*-mPEGMA)$_{CCTP}$	3.5	145	145	91:9
19	(EGPhEA-*co*-mPEGMA)$_{CCTP}$	6.5	204	204	87:13

[a]Aggregates were not detected below the CAC. [b]As the (MAEA-*co*-mPEGMA)$_{CCTP}$ copolymerization ratio was outside an acceptable range limit of between 80:20 and 95:5, it was excluded from the data comparison.

depend on the amount of BzSH present, as would be expected for a reaction under CTA control. However, it should be noted that the final molecular structures differ from the CCTP materials in that a portion of the product will contain a new heteroatom containing the end group (BzS-) and the terminal groups will all be fully saturated. Therefore, there would be no opportunity for post-functionalization/chain transfer with these materials.

2.4. HT Evaluation of CAC. To evaluate the threshold at which the amphiphilic copolymers transition between existing as single chains in solution and becoming nanoaggregates, an assessment of their CAC was conducted. The CAC can also be considered as one of the indicators for micelle stability, which is an important factor when amphiphilic polymers are used as surfactants.[54] However, in practice, collecting data is a labor-intensive and time-consuming activity. Thus, if conventional methodologies were to be adopted, that is, the preparation of stock emulsions/suspensions at the fixed concentration of 500 μg/mL and the subsequent 12 serial dilutions (up to 0.05 μg/mL), for traditional manual nanoprecipitation, this would become a pinch point in any HT pipeline of surfactant design and validation.

Thus, an automated HT method of CAC evaluation was developed and applied. This involved employing a 2D-picoliter piezoelectric inkjet printer (Sciflexarray S5, Scienion) to produce a miniaturized and automated serial dilution system, which utilized a manually pre-prepared stock solution, as described in the experimental section.[55] The advantage of this system dwells in its ability to deliver very small aliquots of the material, precisely. Thus, very low concentrations can be achieved, while avoiding intermediate dilutions. Furthermore, the entire set of the 228 dilution samples could be achieved in just three 96-well plates, vastly reducing the waste from this analysis program. A dynamic light scattering (DLS) plate reader was then used to measure the count rate of each well, which was the result of an average of 10 measurements at a fixed laser power set via the attenuator. A rapid increase in the gradient, when plotting the intensity values at the various explored concentrations as a function of the log values of concentration (μg/mL), allowed the CAC value to be identified (Figure S2.1).[54−56] This increase is due to the change in the intensity of the scattered light from the solutions before and after the micelle/aggregates are formed. In this case, the use of the 3D comb-graft molecular structure of these surfactants led to this transition being less sharply defined than that exhibited by low-molecular-weight surfactants. This is due to monomer pendant groups influencing both the folding of the backbone chain and polymer−polymer interactions. Thus, the CAC values (Table 3) of the 19 amphiphilic copolymers were taken from the intersection of the best fit extrapolated lines as shown in Figure S2.1.

The copolymers from both polymerization techniques (CCTP and thiol-mediated) showed CAC values with the same order of magnitude, suggesting that the copolymer end group did not greatly influence micelle formation. Overall, when the hydrophobic/hydrophilic monomer ratio was similar to the target 90/10 mol/mol (hydrophobic monomer/mPEGMA300), the CAC values were between 3.5 and 22 μg/mL. While there are limited data in the literature quoting pre-measured CAC values, the surfactant literature contains a plethora of quoted and cross-referenced critical micelle concentration (cmc) data. The cmc defines the point at which amphiphilic molecules assemble into larger spherical aggregates, whereas CAC determines the concentration at which premicellar aggregates are formed. Thus, both reflect the point at which molecular self-assembly occurs. Comparison of the data above with the extensive body of literature tabulated cmc values of well-known, commercially available surfactants showed that these values were comparable to those of a range of commercial surfactants, For example, Tween 80 (cmc = 12.0 μg/mL), Brij 30 (4.8 μg/mL), Brij 56 (2.4 μg/mL), Brij 58 (8.4 μg/mL), Brij 76 (3.6 μg/mL), Brij 78 (6.8 μg/mL), and Brij 721 (4.7 μg/mL).[57,58] This suggests that the self-assembling behavior and stability of the resultant micelles

https://doi.org/10.1021/acsami.1c08662
ACS Appl. Mater. Interfaces XXXX, XXX, XXX−XXX

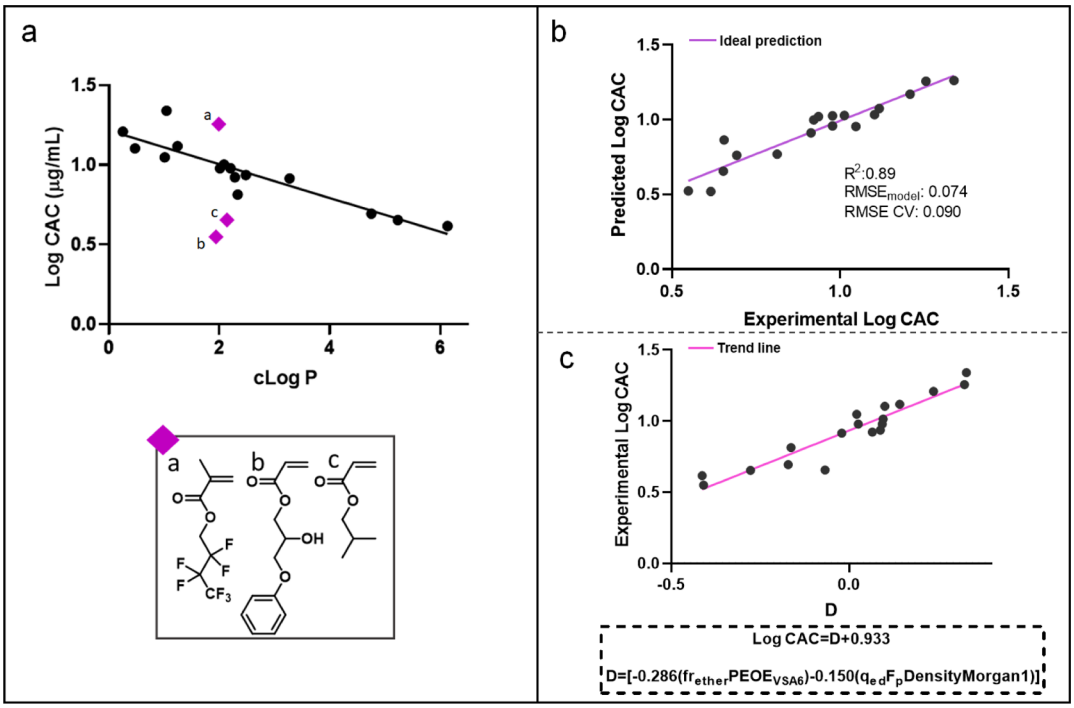

Figure 3. (a) Logarithmic values of the calculated CACs were plotted against the value of the log *P* of 14 hydrophobic monomers. CACs of three surfactants with hydrophobic monomers in the rectangle (a–c) have been excluded from the trend. (b) Experimental log CAC values are plotted against the predicted log CAC values, and performance metrics are shown. (c) Scatter plot showing how the equation fits the data.

could be compared to those of these commercially available surfactants. Furthermore, a review of the data, log CAC versus clog *P* for the hydrophobic monomer monomers, highlighted a general linear downward trend (R^2 0.8304) with the increasing hydrophobic monomer clog *P* values and confirmed that the bulkier monomers led to lower log CACs (Figure 3a).

Finally, we sought to confirm that these CAC values predicted by the HT technique were truly representative of the actual properties of each candidate and not an artifact of the technique. The sizes of the colloidal mixture particles were measured using standard preparation techniques when the systems for each surfactant were below, at, and above the HT-predicted CAC (Table 3). This analysis demonstrated that at a concentration of 0.05 μg/mL, that is, 40 times below the determined CAC of the 18 surfactants, no aggregates were observed. However, once the systems were at or above (i.e., ∼100 μg/mL) the HT predicted values for CAC, the size measurements confirmed the formation of aggregates as their hydrodynamic diameters could be detected via DLS.

While in general terms the relationship between the CAC and log *P* was encouraging, it was clear from the DLS measurements that not all the amphiphilic molecules exhibited as good a correlation. Of the 18 variants explored, one surfactant (F7BMA-*co*-mPEGMA300) appeared to exhibit an overestimation of the CACs when compared to the clog *P* values, whereas two (HPhOPA-*co*-mPEGMA300 and iBuA-*co*-mPEGMA300) presented apparent underestimations of the same property. Thus, it was proposed that the hydrophobic character of the hydrophobic monomers is not the only parameter driving/defining the self-assembling and nano-aggregate stability of these materials.

Such examples of empirical evaluation indicating greater levels of complexity in polymeric quantitative structure–activity relationships have precedent from similar HT-based studies.[59] Furthermore, extended evaluation and cross-referencing of the influence of various molecular descriptors on materials properties have been shown to be capable of developing more exact correlations between the monomer/polymer molecular structure and application performance.[59−61]

Thus, such a computationally based cross-referencing evaluation was conducted using the CAC data obtained in this study in order to resolve the outlying data. To achieve this, the contribution to influence upon the CAC versus log *P* correlation of a broad range of structural features was evaluated *in silico*. These included the potential for bond rotation, physical intermolecular interactions between functional groups, pendant group steric bulk, and so forth.

2.5. Predictive Computational Model Development. Machine Learning Data Analysis was performed by applying a linear multiple regression model using a total number of 20,300 molecular descriptors that considered that all the surfactants possessed the theoretical molar contribution of ∼90/10 mol/mol hydrophobic monomer/mPEGMA300. The experimentally derived data have been shown in Figure 3a, and the model performance has been summarized in Figure 3b,c.

Figure 3b contains the results of a modelling exercise conducted using 18 synthesized surfactants, and it shows that the best performing model provided a correlation value (r^2) of 0.89, a root-mean-squared error (RMSE) of 0.074, and a leave-one-out cross-validation root-mean-squared error (LOOCV RMSE) of 0.090. When this new set of data was compared with the r^2 value (0.83) of the direct experimental comparison, depicted in Figure 3a, a significant improvement in the fit of the data by using the derived model was observed. Furthermore, given that the LOOCV RMSE value is close to RMSE, it is possible to conclude that the generated computational model is sufficiently robust.

https://doi.org/10.1021/acsami.1c08662
ACS Appl. Mater. Interfaces XXXX, XXX, XXX−XXX

To better understand how well the model performs in terms of a "better-than-random prediction", the RMSE value has been compared to the standard deviation of the log CAC value ($\sigma_{\log CAC}$). This comparison is important in order to establish the quality of the performance of the regression linear model. A poor regression would lead to an RMSE that is equivalent to the standard deviation of the log CAC value. In this study, the relationship between these two factors was calculated to be 3.027 (see eq S2.1 in the Supporting Information document for calculations). This suggests that the model performs more than threefold better than a random model.

The relationship shown in Figure 3c is derived by the regression model obtained by multiplying the initial broad set of 200 descriptors by each other and by themselves to widen the feature space, without any research biased, and thus to have access to new combined descriptors. The first combined descriptor is $fr_{ether}PEOE_{VSA6}$, and the second one is *qedFpDensityMorgan1*. The original equation generated by the model is shown in eq 1

$$\log \mathrm{CAC} = -0.286(fr_{ether}{*}PEOE_{VSA6}) - 0.150(qed{*}FpDensityMorgan1) + 0.933 \quad (1)$$

Equation 1: Derived mathematical relationship between log CAC and the linearly combined descriptors.

Consequently, these components of this equation generated by the model can be equated to a linearized relationship (i.e., $y = mx + c$) where $m = 1$; $x = [-0.286(fr_{ether}{*}PEOE_{VSA6}) - 0.150(qed{*}FpDensityMorgan1)]$, and $c = 0.933$.

The descriptors, shown in the predictive equation above, are poorly/weakly cross-correlated. In fact, the r^2 value between the two combined factors (*qedFpDensityMorgan1* and $fr_{ether}PEOE_{VSA6}$) is equal to 0.48, while the single components of *qedFpDensityMorgan1* and $fr_{ether}PEOE_{VSA6}$, alone, show r^2 values of 0.01 and 0.05, respectively. The poor correlation is, again, an underlying indication that the prediction performance of the model is not affected by feature overlapping or redundancy, thus demonstrating its high level of robustness.

In order to give an interpretable molecular meaning to these descriptors, they have been associated to tangible physical features/molecular characteristics of the polymer. This connection is of importance as the ultimate aim is to fully understand how to translate these model data into the molecular design of new polymers with tailored properties. Examples from literature reports define the specific components of the descriptors as follows: (a) $PEOE_{VSA6}$ is a measure of the electrostatic interactions within the molecule,[62] (b) *qed* quantifies the "drug-likeness" of the molecule,[63] (c) fr_{ether} is the number of ether oxygen species in the molecule, and (d) *FpDensityMorgan1* pertains to the influence of steric bulk and the number of heavy atoms present in the structure.[64] In polymer terms, this has been hypothesized to relate to (a) the potential levels of inter-chain interactions, (b) the ability of the hydrophobic monomers to be a hydrogen-bond donator and acceptor, (c) the quantity of the PEG hydrophile that is in the surfactant, and (d) the hydrophobic monomer pendant group steric hindrance and molecular mass.[65] Thus, it has been concluded that the results obtained with this prediction model are very promising, considering the limited number of materials for which practical results existed. These computational findings represent a powerful tool which will enable the rapid and accurate design of a broad range of polymeric surfactants that exhibit both biological functionality and tunable self-assembling features without the need of a wide-ranging screening program.

2.6. CONCLUSIONS

The reported results demonstrate the successful combination of three HT processes to rapidly design, produce, and define the aggregation properties of a library of novel, cell-instructive surface-active polymers. This strategy underpinned the delivery of specific bacterial responses from particle surfaces produced via microfluidic processing. The surfactants are used to both stabilize particle formation and direct the cell-instructive polymer to the surface of the particles as a unimolecular thick coating.[43] Additionally, conducting these operations in a single step maximized the efficiency of the use of the cell-instructive monomers adopted to construct the surfactants and so reduce cost and waste. It also allows the potential for the bulk material properties to be varied independently from the surfactant by simply changing the core monomer that forms the particle.

The strength of applying HT screening and synthesis was successfully demonstrated by the conversion of 20 key bio-instructive functional monomers into comb-graft copolymers suitable for use as a surfactant at small (1 g) and large (10 g) scales within a week. It was enhanced by the successful development of a novel HT strategy to establish the quality of the surfactants produced. A rapid, fully automated method of determining the CAC of these materials was achieved via the use of an inkjet printer at the well plate scale. These data from this property screen were then utilized to build a proof-of-concept computational model to assess the molecular descriptors that identified the four key molecular drivers that underpin the CAC properties of these types of complex, comb-graph, architectural polymers.

Thus, the combination of known HT bioscreening, synthesis techniques and a novel HT inkjet printer-based CAC assay have successfully led to the generation of a range of novel, bio-instructive materials that deliver surface bacterial/cell responses of great interest. This practical strategy, combined with the novel computational assessment of the molecular factors that define surfactant behavior of these complex types of molecular architectures, represents a very powerful tool to allow "on-demand" product/property design from high-performing surfactant materials, such as those required to expand the use of such bio-instructive surfaces into many new biologically driven applications.

■ ASSOCIATED CONTENT

Supporting Information

The Supporting Information is available free of charge at https://pubs.acs.org/doi/10.1021/acsami.1c08662.

Materials; HT reactor configuration; general procedure adopted for the initial parallel polymerization screen contemplating 54 polymerizations using CCTP at a 1.5 g scale; optimization of 10 CCTP parallel polymerizations which exhibited no conversion in the initial screening at a 1.5 g scale; scale-up of four selected parallel polymerizations conducted *via* CCTP from a 1.5 to 10 g scale; general procedure adopted for the parallel polymerization of 12 polymerizations conducted using thiol control agents at a 1.5 g scale; characterization of products from the HT polymer libraries; computational

https://doi.org/10.1021/acsami.1c08662
ACS Appl. Mater. Interfaces XXXX, XXX, XXX−XXX

model; conversion, M_n, $Đ$, and final copolymer ratio of the scale-up reactions with CCTP with a target feed ratio of 90/10 mol/mol; CAC of iBMA-*co*-mPEGMA$_{300}$; CAC plot of intensity of scattered light (kilo counts per second) as a function of concentration (μg/mL) for all the 19 surfactants; and relationship between the standard deviation of the log CAC (σ_{logCAC}) and the RMSE$_{model}$ (PDF)

AUTHOR INFORMATION

Corresponding Authors

Ricky D. Wildman − *Centre for Additive Manufacturing and Department of Chemical and Environmental Engineering, Faculty of Engineering, University of Nottingham, Nottingham NG7 2RD, U.K.;* orcid.org/0000-0003-2329-8471; Email: Ricky.Wildman@nottingham.ac.uk

Benjamin W. Muir − *CSIRO Manufacturing, Clayton 3168 Victoria, Australia;* orcid.org/0000-0002-8858-3217; Email: Ben.Muir@csiro.au

Derek J. Irvine − *Centre for Additive Manufacturing and Department of Chemical and Environmental Engineering, Faculty of Engineering, University of Nottingham, Nottingham NG7 2RD, U.K.;* orcid.org/0000-0003-1461-9851; Email: Derek.Irvine@nottingham.ac.uk

Authors

Valentina Cuzzucoli Crucitti − *Centre for Additive Manufacturing and Department of Chemical and Environmental Engineering, Faculty of Engineering, University of Nottingham, Nottingham NG7 2RD, U.K.*

Leonardo Contreas − *School of Pharmacy, University of Nottingham, Nottingham NG7 2RD, U.K.*

Vincenzo Taresco − *School of Chemistry, University of Nottingham, Nottingham NG7 2RD, U.K.;* orcid.org/0000-0003-4476-8233

Shaun C. Howard − *CSIRO Manufacturing, Clayton 3168 Victoria, Australia*

Adam A. Dundas − *Centre for Additive Manufacturing and Department of Chemical and Environmental Engineering, Faculty of Engineering, University of Nottingham, Nottingham NG7 2RD, U.K.;* orcid.org/0000-0002-7532-5374

Marion J. Limo − *Interface and Surface Analysis Centre, University of Nottingham, Nottingham NG7 2RD, U.K.*

Takasi Nisisako − *Institute of Innovative Research, Tokyo Institute of Technology, Yokohama, Kanagawa 226-8503, Japan;* orcid.org/0000-0003-1724-360X

Philip M. Williams − *School of Pharmacy, University of Nottingham, Nottingham NG7 2RD, U.K.*

Paul Williams − *Biodiscovery Institute, National Biofilms Innovation Centre and School of Life Sciences, University of Nottingham, Nottingham NG7 2RD, U.K.*

Morgan R. Alexander − *School of Pharmacy, University of Nottingham, Nottingham NG7 2RD, U.K.;* orcid.org/0000-0001-5182-493X

Complete contact information is available at: https://pubs.acs.org/10.1021/acsami.1c08662

Author Contributions

V.C.C. carried out the polymer synthesis and CAC assessment laboratory research and wrote the main draft of the manuscript. L.C. and P.M.W. carried out and commented on the theoretical modelling research and contributed to writing of the modelling theory section of the manuscript. V.T. was responsible for the development of the HT CAC methodology and contributed to the manuscript in this section. S.C.H. and B.W.M. were responsible for development and operation of the HT synthesis apparatus and contributed/led to the generation of text for the manuscript in this section. M.J.L. conducted the biophysical analysis of HT DLS and aided in the interpretation. P.W. and M.R.A. provided the conceptualization and rationalization for the background understanding of the monomers and their applications. A.A.D. and T.N. assisted in the design and rationalization of the manuscript for the surfactants design. R.D.W. and D.J.I. generated the concept, led the research process, and contributed to the writing of the manuscript. All the authors contributed to the writing of the manuscript and agreed to the published version of the manuscript.

Notes

The authors declare no competing financial interest.

ACKNOWLEDGMENTS

The authors acknowledge the Manufacturing Biophysics Group (Macromolecular interactions) of CSIRO, especially Dr. Mark Hickey for his consulting for the GPC and Dr. Roger Mulder and his group for the NMR support. This work was supported by the Engineering and Physical Sciences Research Council (grant number EP/N006615/1).

REFERENCES

(1) Magennis, E. P.; Hook, A. L.; Davies, M. C.; Alexander, C.; Williams, P.; Alexander, M. R. Engineering Serendipity: High-Throughput Discovery of Materials That Resist Bacterial Attachment. *Acta Biomater.* **2016**, *34*, 84−92.

(2) Patel, A. K.; Tibbitt, M. W.; Celiz, A. D.; Davies, M. C.; Langer, R.; Denning, C.; Alexander, M. R.; Anderson, D. G. High Throughput Screening for Discovery of Materials That Control Stem Cell Fate. *Curr. Opin. Solid State Mater. Sci.* **2016**, *20*, 202−211.

(3) Hook, A. L.; Anderson, D. G.; Langer, R.; Williams, P.; Davies, M. C.; Alexander, M. R. High Throughput Methods Applied in Biomaterial Development and Discovery. *Biomaterials* **2010**, *31*, 187−198.

(4) Kohn, J. New Approaches to Biomaterials Design. *Nat. Mater.* **2004**, *3*, 745−747.

(5) Hoogenboom, R.; Meier, M. A. R.; Schubert, U. S. Combinatorial Methods, Automated Synthesis and High-Throughput Screening in Polymer Research: Past and Present. *Macromol. Rapid Commun.* **2003**, *24*, 15−32.

(6) Selekman, J. A.; Qiu, J.; Tran, K.; Stevens, J.; Rosso, V.; Simmons, E.; Xiao, Y.; Janey, J. High-Throughput Automation in Chemical Process Development. *Annu. Rev. Chem. Biomol. Eng.* **2017**, *8*, 525−547.

(7) Webster, D. C. Combinatorial and High-Throughput Methods in Macromolecular Materials Lesearch and Development. *Macromol. Chem. Phys.* **2008**, *209*, 237−246.

(8) Nasrullah, M. J.; Webster, D. C. Parallel Synthesis of Polymer Libraries Using Atom Transfer Radical Polymerization (ATRP). *Macromol. Chem. Phys.* **2009**, *210*, 640−650.

(9) Haven, J. J.; Baeten, E.; Claes, J.; Vandenbergh, J.; Junkers, T. High-Throughput Polymer Screening in Microreactors: Boosting the Passerini Three Component Reaction. *Polym. Chem.* **2017**, *8*, 2972−2978.

(10) Rinkenauer, A. C.; Vollrath, A.; Schallon, A.; Tauhardt, L.; Kempe, K.; Schubert, S.; Fischer, D.; Schubert, U. S. Parallel High-Throughput Screening of Polymer Vectors for Nonviral Gene Delivery: Evaluation of Structure-Property Relationships of Transfection. *ACS Comb. Sci.* **2013**, *15*, 475−482.

(11) Burger, B.; Maffettone, P. M.; Gusev, V. V.; Aitchison, C. M.; Bai, Y.; Wang, X.; Li, X.; Alston, B. M.; Li, B.; Clowes, R.; Rankin, N.; Harris, B.; Sprick, R. S.; Cooper, A. I. A Mobile Robotic Chemist. *Nature* **2020**, *583*, 237−241.
(12) Mao, T.; Liu, G.; Wu, H.; Wei, Y.; Gou, Y.; Wang, J.; Tao, L. High Throughput Preparation of UV-Protective Polymers from Essential Oil Extracts via the Biginelli Reaction. *J. Am. Chem. Soc.* **2018**, *140*, 6865−6872.
(13) Mei, Y.; Saha, K.; Bogatyrev, S. R.; Yang, J.; Hook, A. L.; Kalcioglu, Z. I.; Cho, S.-W.; Mitalipova, M.; Pyzocha, N.; Rojas, F.; Van Vliet, K. J.; Davies, M. C.; Alexander, M. R.; Langer, R.; Jaenisch, R.; Anderson, D. G. Combinatorial Development of Biomaterials for Clonal Growth of Human Pluripotent Stem Cells. *Nat. Mater.* **2010**, *9*, 768−778.
(14) Anderson, D. G.; Levenberg, S.; Langer, R. Nanoliter-Scale Synthesis of Arrayed Biomaterials and Application to Human Embryonic Stem Cells. *Nat. Biotechnol.* **2004**, *22*, 863−866.
(15) Patel, A. K.; Celiz, A. D.; Rajamohan, D.; Anderson, D. G.; Langer, R.; Davies, M. C.; Alexander, M. R.; Denning, C. A Defined Synthetic Substrate for Serum-Free Culture of Human Stem Cell Derived Cardiomyocytes with Improved Functional Maturity Identified Using Combinatorial Materials Microarrays. *Biomater.* **2015**, *61*, 257−265.
(16) Vallieres, C.; Hook, A. L.; He, Y.; Crucitti, V. C.; Figueredo, G.; Davies, C. R.; Burroughs, L.; Winkler, D. A.; Wildman, R. D.; Irvine, D. J.; Alexander, M. R.; Avery, S. V.; Irvine, D. J.; Alexander, M. R.; Avery, S. V. Discovery of (Meth)Acrylate Polymers That Resist Colonization by Fungi Associated with Pathogenesis and Biodeterioration. *Sci. Adv.* **2020**, *6*, No. eaba6574.
(17) Hook, A. L.; Chang, C.-Y.; Yang, J.; Luckett, J.; Cockayne, A.; Atkinson, S.; Mei, Y.; Bayston, R.; Irvine, D. J.; Langer, R.; Anderson, D. G.; Williams, P.; Davies, M. C.; Alexander, M. R. Combinatorial Discovery of Polymers Resistant to Bacterial Attachment. *Nat. Biotechnol.* **2012**, *30*, 868−875.
(18) Zhou, Z.; Ruiz Cantu, L.; Chen, X.; Alexander, M. R.; Roberts, C. J.; Hague, R.; Tuck, C.; Irvine, D.; Wildman, R. High-Throughput Characterization of Fluid Properties to Predict Droplet Ejection for Three-Dimensional Inkjet Printing Formulations. *Addit. Manuf.* **2019**, *29*, 100792.
(19) Jeffery, N.; Kalenderski, K.; Dubern, J.; Lomiteng, A.; Dragova, M.; Frost, A.; Macrae, B.; Mundy, A.; Alexander, M.; Williams, P.; Andrich, D. A New Bacterial Resistant Polymer Catheter Coating to Reduce Catheter Associated Urinary Tract Infection (CAUTI): A First-in-Man Pilot Study. *Eur. Urol. Suppl.* **2019**, *18*, No. e377.
(20) Matyjaszewski, K.; Spanswick, J. Controlled/Living Radical Polymerization. *Mater. Today* **2005**, *8*, 26−33.
(21) Zhang, H.; Fijten, M. W. M.; Hoogenboom, R.; Reinierkens, R.; Schubert, U. S. Application of a Parallel Synthetic Approach in Atom-Transfer Radical Polymerization: Set-Up and Feasibility Demonstration. *Macromol. Rapid Commun.* **2003**, *24*, 81−86.
(22) Cosson, S.; Danial, M.; Saint-Amans, J. R.; Cooper-White, J. J. Accelerated Combinatorial High Throughput Star Polymer Synthesis via a Rapid One-Pot Sequential Aqueous RAFT (Rosa-RAFT) Polymerization Scheme. *Macromol. Rapid Commun.* **2017**, *38*, 1600780.
(23) Heuts, J. P. A.; Muratore, L. M.; Davis, T. P. Preparation and Characterization of Oligomeric Terpolymers of Styrene, Methyl Methacrylate and 2-Hydroxyethyl Methacrylate: A Comparison of Conventional and Catalytic Chain Transfer. *Macromol. Chem. and Phys.* **2000**, *201*, 2780−2788.
(24) Sanders, G. C.; Duchateau, R.; Lin, C. Y.; Coote, M. L.; Heuts, J. P. A. End-Functional Styrene-Maleic Anhydride Copolymers via Catalytic Chain Transfer Polymerization. *Macromolecules* **2012**, *45*, 5923−5933.
(25) Suddaby, K. G.; Haddleton, D. M.; Hastings, J. J.; Richards, S. N.; O'Donnell, J. P. Catalytic Chain Transfer for Molecular Weight Control in the Emulsion Polymerization of Methyl Methacrylate and Methyl Methacrylate - Styrene. *Macromol.* **1996**, *29*, 8083−8091.
(26) Atkins, C. J.; Patias, G.; Town, J. S.; Wemyss, A. M.; Eissa, A. M.; Shegiwal, A.; Haddleton, D. M. A Simple and Versatile Route to Amphiphilic Polymethacrylates: Catalytic Chain Transfer Polymerisation (CCTP) Coupled with Post-Polymerisation Modifications. *Polym. Chem.* **2019**, *10*, 646−655.
(27) Lowe, A. B. Thiol-Ene "Click" Reactions and Recent Applications in Polymer and Materials Synthesis. *Polym. Chem.* **2010**, *1*, 17−36.
(28) Gridnev, A. A.; Ittel, S. D. Catalytic Chain Transfer in Free-Radical Polymerizations. *Chem. Rev.* **2001**, *101*, 3611−3660.
(29) Heuts, J. P. A.; Smeets, N. M. B. Catalytic Chain Transfer and Its Derived Macromonomers. *Polym. Chem.* **2011**, *2*, 2407.
(30) Engelis, N. G.; Anastasaki, A.; Nurumbetov, G.; Truong, N. P.; Nikolaou, V.; Shegiwal, A.; Whittaker, M. R.; Davis, T. P.; Haddleton, D. M. Sequence-Controlled Methacrylic Multiblock Copolymers via Sulfur-Free RAFT Emulsion Polymerization. *Nat. Chem.* **2017**, *9*, 171−178.
(31) Raffa, P.; Wever, D. A. Z.; Picchioni, F.; Broekhuis, A. A. Polymeric Surfactants: Synthesis, Properties, and Links to Applications. *Chem. Rev.* **2015**, *115*, 8504−8563.
(32) Czajka, A.; Hazell, G.; Eastoe, J. Surfactants at the Design Limit. *Langmuir* **2015**, *31*, 8205−8217.
(33) Kakde, D.; Taresco, V.; Bansal, K. K.; Magennis, E. P.; Howdle, S. M.; Mantovani, G.; Irvine, D. J.; Alexander, C. Amphiphilic Block Copolymers from a Renewable ϵ-Decalactone Monomer: Prediction and Characterization of Micellar Core Effects on Drug Encapsulation and Release. *J. Mater. Chem. B* **2016**, *4*, 7119−7129.
(34) Tizzotti, M. J.; Sweedman, M. C.; Schäfer, C.; Gilbert, R. G. The Influence of Macromolecular Architecture on the Critical Aggregation Concentration of Large Amphiphilic Starch Derivatives. *Food Hydrocoll* **2013**, *31*, 365−374.
(35) La Sorella, G.; Strukul, G.; Scarso, A. Recent Advances in Catalysis in Micellar Media. *Green Chem.* **2015**, *17*, 644−683.
(36) Blanazs, A.; Armes, S. P.; Ryan, A. J. Self-Assembled Block Copolymer Aggregates: From Micelles to Vesicles and Their Biological Applications. *Macromol. Rapid Commun.* **2009**, *30*, 267−277.
(37) Torchilin, V. P. Structure and Design of Polymeric Surfactant-Based Drug Delivery Systems. *J. Controlled Release* **2001**, *73*, 137−172.
(38) Mulligan, C. N. Environmental Applications for Biosurfactants. *Environ. Pollut.* **2005**, *133*, 183−198.
(39) Banat, I. M.; Makkar, R. S.; Cameotra, S. S. Potential commercial applications of microbial surfactants. *Appl. Microbiol. Biotechnol.* **2000**, *53*, 495−508.
(40) Adlington, K.; Nguyen, N. T.; Eaves, E.; Yang, J.; Chang, C.-Y.; Li, J.; Gower, A. L.; Stimpson, A.; Anderson, D. G.; Langer, R.; Davies, M. C.; Hook, A. L.; Williams, P.; Alexander, M. R.; Irvine, D. J. Application of Targeted Molecular and Material Property Optimization to Bacterial Attachment-Resistant (Meth)Acrylate Polymers. *Biomacromol.* **2016**, *17*, 2830−2838.
(41) Sanni, O.; Chang, C. Y.; Anderson, D. G.; Langer, R.; Davies, M. C.; Williams, P. M.; Williams, P.; Alexander, M. R.; Hook, A. L. Bacterial Attachment to Polymeric Materials Correlates with Molecular Flexibility and Hydrophilicity. *Adv. Healthc. Mater.* **2015**, *4*, 695−701.
(42) Hook, A. L.; Chang, C.-Y.; Yang, J.; Luckett, J.; Cockayne, A.; Atkinson, S.; Mei, Y.; Bayston, R.; Irvine, D. J.; Langer, R.; Anderson, D. G.; Williams, P.; Davies, M. C.; Alexander, M. R. Combinatorial Discovery of Polymers Resistant to Bacterial Attachment. *Nat. Biotechnol.* **2012**, *30*, 868−875.
(43) Dundas, A. A.; Cuzzucoli Crucitti, V.; Haas, S.; Dubern, J. F.; Latif, A.; Romero, M.; Sanni, O.; Ghaemmaghami, A. M.; Williams, P.; Alexander, M. R.; Wildman, R.; Irvine, D. J. Achieving Microparticles with Cell-Instructive Surface Chemistry by Using Tunable Co-Polymer Surfactants. *Adv. Funct. Mater.* **2020**, *30*, 2001821.
(44) Celiz, A. D.; Smith, J. G. W.; Patel, A. K.; Hook, A. L.; Rajamohan, D.; George, V. T.; Flatt, L.; Patel, M. J.; Epa, V. C.; Singh,

https://doi.org/10.1021/acsami.1c08662
ACS Appl. Mater. Interfaces XXXX, XXX, XXX−XXX

T.; Langer, R.; Anderson, D. G.; Allen, N. D.; Hay, D. C.; Winkler, D. A.; Barrett, D. A.; Davies, M. C.; Young, L. E.; Denning, C.; Alexander, M. R. Discovery of a Novel Polymer for Human Pluripotent Stem Cell Expansion and Multilineage Differentiation. *Adv. Mater.* **2015**, *27*, 4006−4012.
(45) Varnek, A.; Gaudin, C.; Marcou, G.; Baskin, I.; Pandey, A. K.; Tetko, I. V. Inductive Transfer of Knowledge: Application of Multi-Task Learning and Feature Net Approaches to Model Tissue-Air Partition Coefficients. *J. Chem. Inf. Model.* **2009**, *49*, 133−144.
(46) Taresco, V.; Suksiriworapong, J.; Styliari, I. D.; Argent, R. H.; Swainson, S. M. E.; Booth, J.; Turpin, E.; Laughton, C. A.; Burley, J. C.; Alexander, C.; Garnett, M. C. New N-Acyl Amino Acid-Functionalized Biodegradable Polyesters for Pharmaceutical and Biomedical Applications. *RSC Adv.* **2016**, *6*, 109401−109405.
(47) Kolitz, M.; Cohen-Arazi, N.; Hagag, I.; Katzhendler, J.; Domb, A. J. Biodegradable Polyesters Derived from Amino Acids. *Macromol.* **2009**, *42*, 4520−4530.
(48) Biasutti, J. D.; Evan Roberts, G.; Lucien, F. P. Substituent Effects in the Catalytic Chain Transfer Polymerization of 2-Hydroxyethyl Methacrylate. *Eur. Polym. J.* **2003**, *39*, 429−435.
(49) Haddleton, D. M.; Depaquis, E.; Kelly, E. J.; Kukulj, D.; Morsley, S. R.; Bon, S. A. F.; Eason, M. D.; Steward, A. G. CCTP in Water and Water/Alcohol Solution. *Polym. Sci. Part A Polym. Chem.* **2001**, *39*, 2378−2384.
(50) Haddleton, D. M.; Maloney, D. R.; Suddaby, K. G. Competition between β-Scission of Macromonomer-Ended Radicals and Chain Transfer to Cobalt(II) in Catalytic Chain Transfer Polymerization (CCTP). *Macromolecules* **1996**, *29*, 481−483.
(51) Patias, G.; Wemyss, A. M.; Efstathiou, S.; Town, J. S.; Atkins, C. J.; Shegiwal, A.; Whitfield, R.; Haddleton, D. M. Controlled Synthesis of Methacrylate and Acrylate Diblock Copolymers: Via End-Capping Using CCTP and FRP. *Polym. Chem.* **2019**, *10*, 6447−6455.
(52) Heuts, J. P. A.; Forster, D. J.; Davis, T. P. Effects of Ester Chain Length and Temperature on the Catalytic Chain Transfer Polymerization of Methacrylates. *Macromol.* **1999**, *32*, 3907−3912.
(53) Izunobi, J. U.; Higginbotham, C. L. Polymer Molecular Weight Analysis by 1H NMR Spectroscopy. *J. Chem. Educ.* **2011**, *88*, 1098−1104.
(54) Roldo, M.; Power, K.; Smith, J. R.; Cox, P. A.; Papagelis, K.; Bouropoulos, N.; Fatouros, D. G. N-Octyl-O-Sulfate Chitosan Stabilises Single Wall Carbon Nanotubes in Aqueous Media and Bestows Biocompatibility. *Nanoscale* **2009**, *1*, 366.
(55) Styliari, I. D.; Conte, C.; Pearce, A. K.; Hüsler, A.; Cavanagh, R. J.; Limo, M. J.; Gordhan, D.; Nieto-Orellana, A.; Suksiriworapong, J.; Couturaud, B.; Williams, P.; Hook, A. L.; Alexander, M. R.; Garnett, M. C.; Alexander, C.; Burley, J. C.; Taresco, V. High-Throughput Miniaturized Screening of Nanoparticle Formation via Inkjet Printing. *Macromol. Mater. Eng.* **2018**, *303*, 1800146.
(56) Cheng, W.; Rajendran, R.; Ren, W.; Gu, L.; Zhang, Y.; Chuang, K.-H.; Liu, Y. A Facile Synthetic Approach to a Biodegradable Polydisulfide MRI Contrast Agent. *J. Mater. Chem. B* **2014**, *2*, 5295−5301.
(57) Hait, S. K.; Moulik, S. P. Determination of Critical Micelle Concentration (CMC) of Nonionic Surfactants by Donor-Acceptor Interaction with Iodine and Correlation of CMC with Hydrophile-Lipophile Balance and Other Parameters of the Surfactants. *J. Surfactants Deterg.* **2001**, *4*, 303−309.
(58) Patist, A.; Bhagwat, S. S.; Penfield, K. W.; Aikens, P.; Shah, D. O. On the Measurement of Critical Micelle Concentrations of Pure and Technical-Grade Nonionic Surfactants. *J. Surfactants Deterg.* **2000**, *3*, 53−58.
(59) Dundas, A. A.; Sanni, O.; Dubern, J. F.; Dimitrakis, G.; Hook, A. L.; Irvine, D. J.; Williams, P.; Alexander, M. R. Validating a Predictive Structure−Property Relationship by Discovery of Novel Polymers Which Reduce Bacterial Biofilm Formation. *Adv. Mater.* **2019**, *31*, 1903513.
(60) Sanni, O.; Chang, C. Y.; Anderson, D. G.; Langer, R.; Davies, M. C.; Williams, P. M.; Williams, P.; Alexander, M. R.; Hook, A. L. Bacterial Attachment to Polymeric Materials Correlates with Molecular Flexibility and Hydrophilicity. *Adv. Healthc. Mater.* **2015**, *4*, 695−701.
(61) Dundas, A. A.; Hook, A. L.; Alexander, M. R.; Kingman, S. W.; Dimitrakis, G.; Irvine, D. J. Methodology for the Synthesis of Methacrylate Monomers Using Designed Single Mode Microwave Applicators. *React. Chem. Eng.* **2019**, *4*, 1472−1476.
(62) Labute, P. A. Widely Applicable Set of Descriptors. *J. Mol. Graph. Model.* **2000**, *18*, 464−477.
(63) Bickerton, G. R.; Paolini, G. V.; Besnard, J.; Muresan, S.; Hopkins, A. L. Quantifying the Chemical Beauty of Drugs. *Nat. Chem.* **2012**, *4*, 90−98.
(64) Rogers, D.; Hahn, M. Extended-Connectivity Fingerprints. *J. Chem. Inf. Model.* **2010**, *50*, 742−754.
(65) A. Decade of Drug-Likeness. *Nat. Rev. Drug Discovery*. Nature Publishing Group November **2007**, *6* p 853. DOI: DOI: 10.1038/nrd2460.

https://doi.org/10.1021/acsami.1c08662
ACS Appl. Mater. Interfaces XXXX, XXX, XXX−XXX